

Evaluation of the QUIC Pressure Solver using wind-tunnel data from single and multi-building experiments

Akshay Gowardhan¹, Michael Brown², Mathew Nelson²,
David DeCroix² and Eric Pardyjak¹

¹University of Utah, Salt Lake City, Utah

²Los Alamos National Laboratory, Los Alamos, New Mexico

1. INTRODUCTION

The QUIC (Quick Urban & Industrial Complex) fast response dispersion modeling system produces high-resolution wind and concentration fields in cities. It consists of an urban wind model QUIC-URB, a Lagrangian dispersion model QUIC-PLUME, and a graphical user interface QUIC-GUI. Such models, which can quickly produce the required velocity and concentration fields, have many applications, especially for cases where turnaround time is very important. In cases of accidental or deliberate release of chemical, biological and radiological (CBR) agents in an urban area, it is important to estimate the amount of infiltration of harmful substances into the surrounding buildings. The first step in the process would be to predict pressure on building surfaces.

Many fast response models do not predict the wind field by solving the momentum equation, but are based on empirical/ diagnostic methods. Therefore such models do not predict the pressure field while solving for the wind field. QUIC-URB generates a mass consistent mean wind field around buildings by using various empirical relationships to initialize the velocity fields in the regions around buildings (e.g. *upwind cavity, wake, street canyon, and rooftop*). This initial flow field is then forced to satisfy mass conservation (see Fig.1).

As part of the Quick Urban & Industrial Complex (QUIC) Dispersion Modeling System, a pressure solver has been developed to compute a 3D pressure field estimate around buildings. The solver generates the pressure field by solving the pressure Poisson equation, obtained by taking the spatial divergence of the steady-state Navier-Stokes equations for incompressible flows. The input to the solver is the 3D mean wind field obtained from the QUIC-URB fast response urban wind model (Pardyjak and Brown 2001).

2. MODEL DESCRIPTION AND SOLUTION PROCEDURE

The pressure Poisson equation is derived from the Reynolds-averaged Navier-Stokes (RANS) equations for incompressible flow without body

forces, expressed here using Einsteinian notation as:

$$\frac{\partial \bar{U}_i}{\partial t} = -\frac{\partial(\bar{U}_i \bar{U}_j)}{\partial x_j} - \frac{1}{\rho} \frac{\partial \bar{P}}{\partial x_i} - \frac{\partial(\bar{u}'_i \bar{u}'_j)}{\partial x_j} + \nu \frac{\partial^2 \bar{U}_i}{\partial x_j \partial x_j} \quad (1)$$

where \bar{U}_i is the mean velocity in the x_i direction, u'_i is the turbulent fluctuating velocity, \bar{P} is the mean pressure, ρ is the average density, $\bar{u}'_i \bar{u}'_j$ is the Reynolds stress, and ν is the kinematic viscosity.

Assuming steady-state conditions and taking the divergence of Eqn. (1), we obtain

$$\frac{\partial}{\partial x_i} \left(\frac{\partial \bar{P}}{\partial x_i} \right) = \rho \frac{\partial}{\partial x_i} \left(\nu \frac{\partial^2 \bar{U}_i}{\partial x_j \partial x_j} - \frac{\partial(\bar{U}_i \bar{U}_j)}{\partial x_j} - \frac{\partial(\bar{u}'_i \bar{u}'_j)}{\partial x_j} \right) \quad (2)$$

Equation (2) is the pressure Poisson equation. Since the QUIC-URB wind model only produces the mean wind field and produces no information on the turbulence, for the time being, we simplify the equation further by neglecting the Reynolds stresses. As will be discussed later, differences between the model-computed and measured pressure may be due to neglecting these terms. In the future, the Reynolds stresses will be included in the calculation to study the effect of turbulence on the mean pressure distribution on building surfaces.

The QUIC Pressure Solver uses the Jacobi method to iteratively solve the pressure Poisson equation. A second-order accurate *central differencing* scheme has been used to obtain the source term for the pressure Poisson equation (R.H.S. of Eqn. (2)) at each grid point in the solution domain. At the west and south building faces, a first-order accurate *upwind differencing* scheme is used to calculate the source term and at the east and north faces, a first-order accurate *forward differencing* scheme is used.

At the building faces, the pressure field is obtained by solving the steady-state Reynolds-averaged Navier-Stokes equation in the direction normal to the wall. For example, for the face

* Corresponding author address: Akshay Gowardhan,
University of Utah, Salt Lake City
UT-87545, e-mail: aagowardhan@yahoo.com

normal to the x-direction, the pressure field is obtained by solving:

$$\frac{\partial \bar{P}}{\partial x} = \rho \left(-\frac{\partial \bar{U}\bar{U}}{\partial x} - \frac{\partial \bar{U}\bar{V}}{\partial y} - \frac{\partial \bar{U}\bar{W}}{\partial z} + \nu \left[\frac{\partial^2 \bar{U}}{\partial x^2} + \frac{\partial^2 \bar{U}}{\partial y^2} + \frac{\partial^2 \bar{U}}{\partial z^2} \right] \right) \quad (3)$$

The initial value of pressure at each grid point inside the solution domain was specified as the ambient atmospheric pressure. The boundary value was set to atmospheric pressure i.e., Dirichlet boundary condition.

The computed pressure field is normalized by subtracting the ambient atmospheric pressure (P_o) and then by dividing by the free stream velocity (V_o) at the reference height to obtain the coefficient of pressure (C_p):

$$C_p = \frac{\bar{P} - P_o}{\left(\frac{1}{2} \rho V_o^2\right)} \quad (4)$$

3. EXPERIMENTAL DESCRIPTION

The QUIC Pressure Solver has been evaluated using wind-tunnel data from a cube, a tall building, a low building with large footprint, and multiple building experiments. Comparisons were made with the wind tunnel data of Baines (1963) for a cubical building and a tall building with dimensions of 1:1:8 (length: width: height). The validation for a low - flat building 1:1:0.5 (length: width: height) is done using experimental data obtained from Architectural Institute of Japan(AIJ) report (1998) and the multiple building case of 7x1 2D array of buildings was compared to experimental data obtained from the experiments carried out in the U.S. Environmental Protection Agency's (EPA) fluid modeling facility maintenance (Brown et a. 2001)

The wind-tunnel experiments of Baines (1963) were performed in the low-speed open-return wind tunnel at the Department of Mechanical Engineering at the University of Toronto. The tunnel has a cross-sectional area of 1.33 m by 2.67 m and a maximum speed of 8.33 m/sec. The model of the building was made of acrylic plastic sheet material. The cubical and tall building had a square floor plan and a height-to-width ratio of 1:1 and 1:8, respectively (Baines 1963). Pressures were small and required the careful use of a micro manometer.

The experiments were conducted with uniform flow and boundary-layer flow. For the case of sheared flow, a boundary-layer velocity profile was produced in the lower half of the wind tunnel by installing a curved screen in the entrance of the wind-tunnel test section. The shear inflow is

represented by a power law with an exponent of 0.25:

$$u = u_{ref} \left(\frac{z}{z_{ref}} \right)^{0.25} \quad (5)$$

In this work, comparison is done only for the sheared inflow case as this kind of flow is observed is most urban areas.

Unfortunately, details of the experimental work done by Architectural Institute of Japan (AIJ) were not documented in the reports, but it was mentioned that the inflow profile produced was a power-law shear-layer profile with exponent of 0.25.

The experimental data for a 2D array of 7x1 buildings were obtained from the experiments carried out in the U.S. Environmental Protection Agency's (EPA) fluid modeling facility maintenance (Brown et al. 2001).

The 2D array consisted of 7 x 1 buildings (0.15 x 3.7 x 0.15m) with one H spacing. With S/H ratios of the street canyon as one (S= Length of street canyon and H= Height of the street canyon), the 2D arrays should be somewhere between the skimming and wake interference flow regimes (Oke 1987). The building models were placed in a simulated neutral atmospheric boundary layer with a depth of 1.8m, a roughness length of 1mm, and a power law exponent of 0.16. The distance of the array from the leading edge of spires was 10.9m to allow sufficient upstream fetch for the boundary layer to grow to equilibrium

4. RESULTS AND DISCUSSION

4.1. Flow over cubical building

To match the Baines shear-flow experiment, a power-law inlet velocity profile was specified in the QUIC simulation (see Eqn. (5)). The reference velocity u_{ref} at building height was set to 5m/s. The value of the power-law index n was taken as 0.25. The rooftop recirculation (Bagal et al. 2004) and the upwind cavity (Bagal et al. 2005) flags were turned on in the QUIC-URB wind model. The grid cell size was again set to H/10. The reference height for normalizing pressure was again taken as the building height (H).

Figure 2 shows the pressure coefficient contours generated by the QUIC Pressure Solver on the building surfaces and Figure 3 shows the wind-tunnel measurements (Baines, 1963). The predicted and measured C_p on the front face has a somewhat similar spatial distribution, although there are some significant differences especially

over the lower half of the building face. The maximum value on the front face is under predicted by about 15% and is found higher up on the building face. The differences on the lower half of the building front face may result from the pressure solver neglecting the Reynolds stresses which have high gradients there. In addition, the differences may be due to differences between the model-produced and measured mean wind in the upwind cavity zone.

On the rooftop, the model-computed and measured C_p both vary from large negative values just downwind of the leading edge and increase as the back edge is approached. The model computations tend to have stronger spatial gradients near the leading and back edges and weaker spatial gradients in the middle of the roof. The maximum pressure deficit found near the leading edge is over predicted by about 25%, while positive values are found in the model solution near the back edge in contrast to the negative values obtained in the measurements.

As previously mentioned, due to QUIC-URB not producing sidewall recirculation zones, we expect significant differences between model-computed and measured C_p values. Larger pressure deficits are found in the measurements, with C_p values being about 2-4 times those predicted by the pressure solver.

The pressure deficit computed by the QUIC Pressure Solver on the back wall is substantially larger as compared to the experimental data. The predicted values show a variation from -0.5 to -0.35 on the back wall whereas the measured values have a more uniform value of -0.2 on the back wall. This can be explained by the fact that the parameterization for wake cavity in QUIC-URB produces significantly stronger velocities at the top-back face of the building (Pardyjak and Brown 2001).

From Gowardhan et al. (2005), it was observed that even Advanced CFD technique like LES are also not in complete agreement with experimental data.

4.2. Flow over tall building

Figure 4 shows the contours of the pressure coefficient generated by the QUIC Pressure Solver on the building surfaces and Figure 5 shows the wind-tunnel measurements for the same case (Baines 1963). For the front face, it can be seen that the spatial distribution of C_p is similar, but the maximum value is over predicted by about 10%.

The predicted values on the rooftop and sidewalls are not in agreement with the observed

values. The sidewall differences are again most likely a result of the lack of a parameterization that captures the physics of flow separating of the building sides. The rooftop differences may be due to differences in the nature of the rooftop recirculation mean wind field predicted by QUIC-URB or due to the strong turbulence expected here which is not accounted for in the QUIC Pressure Solver.

In spite of the large turbulence gradients in the recirculating region at the back wall, the predicted values are in fair agreement with the wind tunnel data in the top and lower part of the back face. Though, in the middle part of the back face, the solver under predicts the values by around 40%. This may be again because of higher velocities predicted on the back face by QUIC-URB.

4.3. Flow over low flat building

A power law profile has been used as the inlet profile for a sheared flow over a low flat building.

Figure 6 shows the contours of coefficient of mean pressure generated by QUIC pressure solver on the building surfaces and Figure 7 shows the wind tunnel measurements for the same case (AIJ).

It is observed that the predicted values on front face are in fair good agreement with the wind tunnel data. On the back wall, it is again observed that the model under predicts the C_p by 30%. This is most likely due to overestimation of velocity by QUIC-URB in the wake parameterization. The values on the side faces are substantially higher than the experimental value. This can be again explained due to lack of parameterization for side wall recirculation. However on the roof of the building it was observed that the model performed reasonably well on the front half of the roof, but on the later have the model predicted substantially high value of C_p . This may be due to improper rooftop parameterization done in QUIC-URB which sudden increase in velocity after the reattachment point on the rooftop.

4.4. Flow over 2D array of 7x1 buildings

Figure 7 shows the predicted value of C_p along the centerline of the buildings for a sheared flow over a 2D array of 7x1 buildings. The coefficient of pressure was calculated by normalizing the gauge pressure by the free stream velocity at the roof of the wind tunnel (4.23m/s).

Figure 8 shows the wind tunnel value of C_p for the same case. The wind tunnel data shows that the value of C_p in the first street canyon and the other street canyons is different. The QUIC

pressure solver predicts nearly same value for all the street canyons because QUIC-URB does not differentiate between various street canyons and has same parameterization for all of them.

The results indicate that the values of C_p predicted by QUIC Pressure Solver on the top faces of the buildings are in reasonable agreement with the experimental data. For the front and back faces of the buildings, the solver is able to predict the nature of C_p fairly well but quantitatively, the predicted values are off by a factor of two which also implies that the street canyon parameterization in QUIC-URB produced lower velocities as compared to the experimental data. On the rooftop of the first building, the model compares fairly well with the measurements, however for all other rooftops, the model significantly under predicts the value of C_p as on the top of these buildings, rooftop recirculation will not be formed, but QUIC-URB still produces rooftop recirculation for these buildings.

The reasons for above mentioned deficiencies maybe because the QUIC-URB wind parameterizations were developed for 3D flow for buildings with finite H/W ratio.

5. CONCLUSION

In this paper, we have compared the pressure coefficient C_p computed by the QUIC Pressure Solver to experimental measurements on a cube, a tall building, a low-flat building and a case of multiple buildings(2d array of 7x1 buildings) for sheared flow normal to face of the building. It has been observed that the model-computed C_p for the single building configurations were in reasonably good agreement with the experimental data on the upwind face of the buildings in spite of neglecting the Reynolds stresses in the pressure solver. This is because the pressure gradients in this region are mostly dominated by the mean inflow.

The mean pressure values computed by the model on the rooftop face are in fair agreement with the experimental data. The model clearly shows a large pressure deficit on the windward side of the rooftop which is due to separation and suction caused by rooftop recirculation and the negative pressure decreases as we go from the windward side to leeward side.

The predicted values of C_p on the back face of the building are not consistent with the experimental data. However, there are also significant differences between experimental data from two different sources and results from LES simulations (Gowardhan et. al, 2005).

The model is not able to predict C_p correctly on the sidewalls of the building due to the lack of a side-wall recirculation zone in the QUIC-URB wind model. The model appears to perform slightly better for the oblique wind angle case and for the shear inflow case.

In the multiple buildings case, the differences between predicted and experimental values of C_p can be attributed to the fact that the QUIC-URB parameterization was done for 3D flow and the experimental data available was for a 2D flow. Also, improvement in the pressure solution is expected with better parameterization of street canyon region.

In summary, the mean pressure coefficient predicted by the QUIC Pressure Solver is in fair to reasonable agreement on the front and rooftop faces for different configuration of single building, in worse agreement on the back face, and in poor agreement on the side face. It is expected that if the mean wind fields computed by the QUIC-URB model are improved that the pressure solutions will also improve. QUIC-URB is currently undergoing testing and evaluation and a side-wall recirculation algorithm is planned to be implemented in the near future. We also intend to investigate the effects of neglecting the Reynolds stresses in our calculations and to ascertain what sorts of errors are acceptable for emergency response applications, for example, outdoor-to-indoor infiltration.

6. REFERENCES

Architectural Institute of Japan, 1998: Numerical prediction of wind loading on buildings and structures.

ASHRAE Handbook of Fundamentals, 1985 ed., p. 14.4, American Society of Heating, Refrigerating and Air-Conditioning Engineers, Inc., Atlanta, GA, 1985

Bagal N.L., B. Singh, E.R. Pardyjak and M.J. Brown, 2004: Implementation of rooftop recirculation parameterization in the QUIC fast response urban wind model, Fifth Symposium on the Urban Environment, Vancouver, BC, August 23-26 2004.

Bagal, N., Pardyjak, E.R., Brown, M.J., 2004: Improved Upwind Cavity Parameterization for a Fast Response Urban Wind Model, Joint URBAN2003 Street Canyon Experiment, 84th Annual AMS Meeting, Seattle, WA, January 11-15 2004.

Baines, W.D., 1963: Effects of velocity distribution on wind loads and flow patterns on buildings. *The symposium on wind effects on*

buildings and structure, Middlesex, England, National Physical Lab. **1**, 197-225.

Gowardhan, A.A., Brown, M.J. and DeCroix, D.S., 2005: QUIC Pressure Solver- *A technical Report*, Los Alamos National Laboratory, Los Alamos, NM.

Pardjak, E.R., N. L. Bagal and M. J. Brown, 2003: Improved velocity deficit parameterizations for a fast response urban wind model, AMS Conf. on Urban Zone, Seattle, WA, LA-UR-03-8512.

Pardjak, E.R. and M.J. Brown, 2001: Evaluation of a Fast-Response Urban Wind Model-Comparison to Single-Building Wind Tunnel Data. Los Alamos National Laboratory report LA-UR-01-4028.

Rehm, R.G., McGrattan, K.B., Baum, H.R. and Simiu E., 1999: An efficient large eddy simulation algorithm for computational wind engineering: Application of surface pressure computation on a single building.. National Institute of Standards and Technology report NISTIR 6371.

Röckle, R., 1990: Bestimmung der Stromungsverhältnisse im Bereich Komplexer Bebauungsstrukturen. Ph.D. thesis, *Vom Fachbereich Mechanik, der Technischen Hochschule Darmstadt*, Germany.

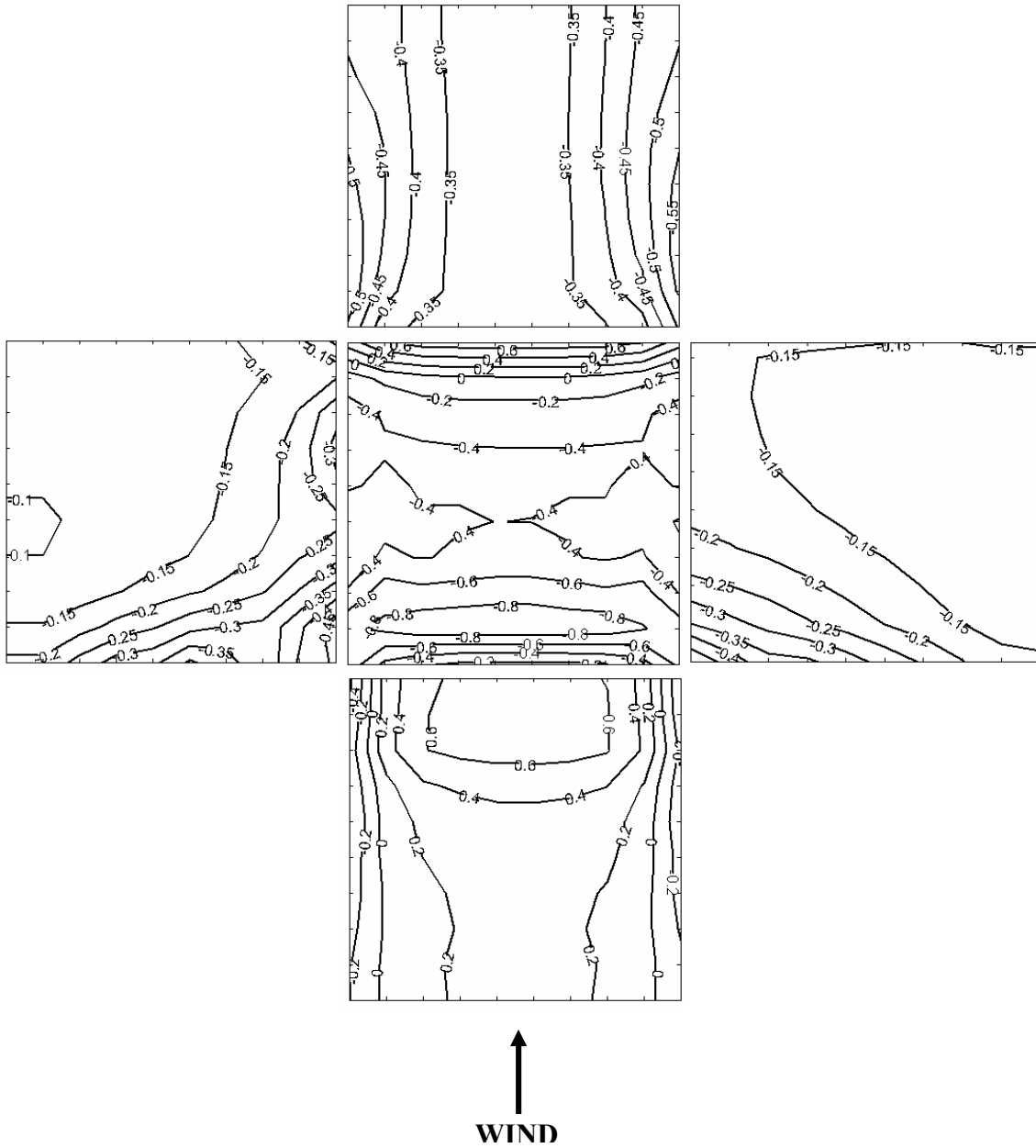


Fig. 1: Pressure coefficient produced by the QUIC Pressure Solver on a cubical building for a shear inflow perpendicular to the building face.

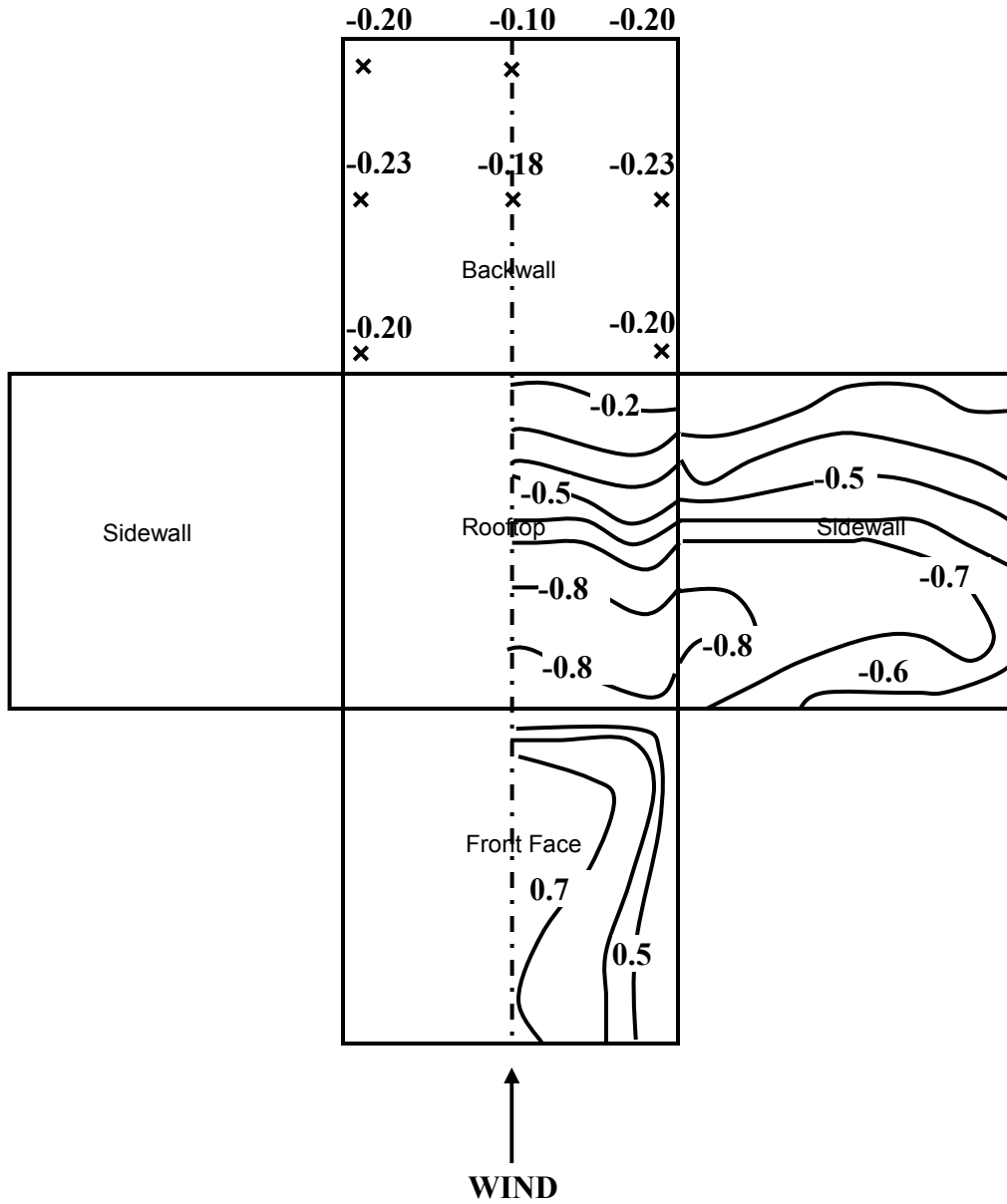


Fig. 2: Wind-tunnel measurements of the pressure coefficient on a cubical building for a shear inflow perpendicular to the building face (modified from Baines, 1963).

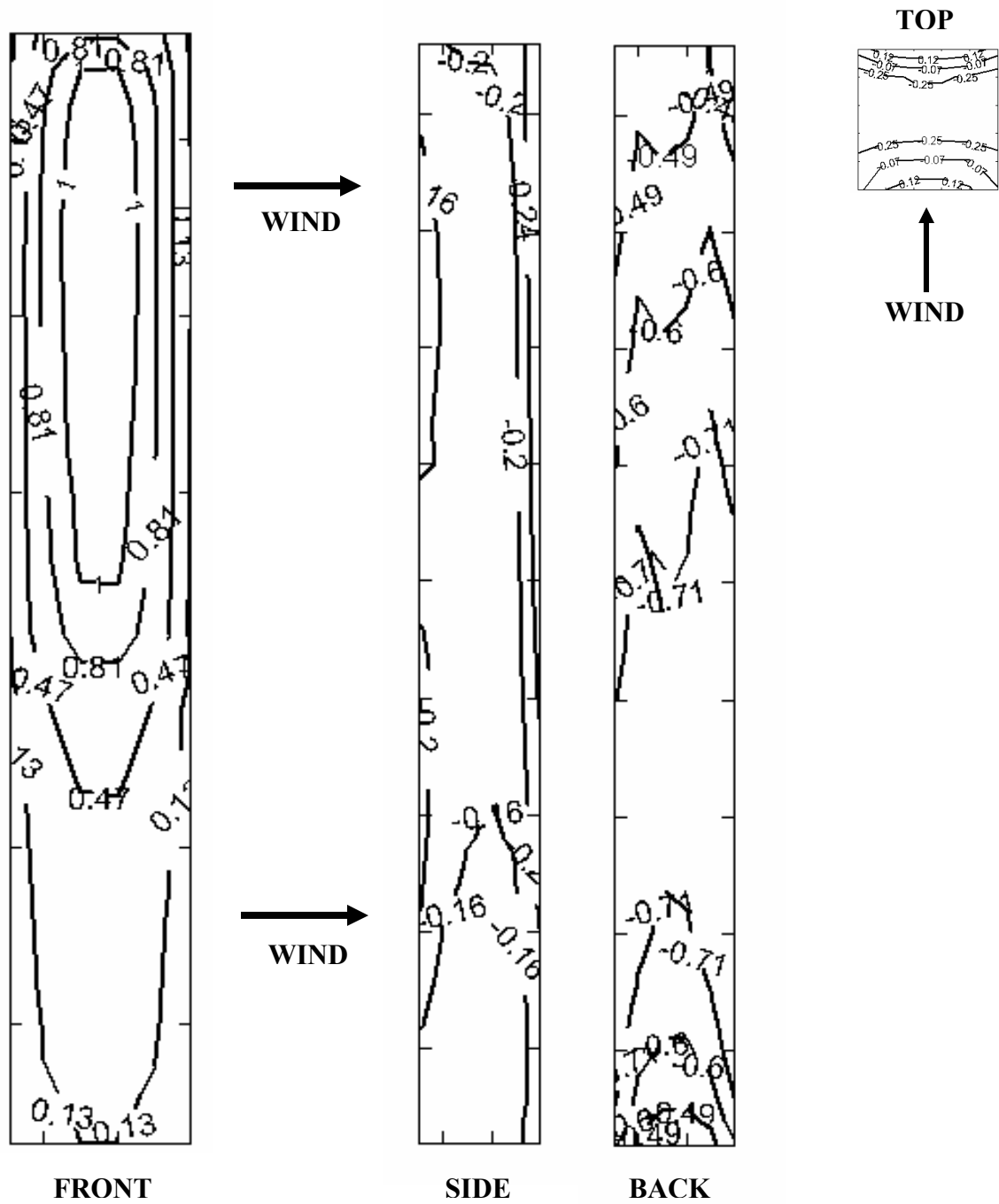


Fig. 3: Pressure coefficient produced by the QUIC Pressure Solver on a tall building for a shear inflow perpendicular to the building face.

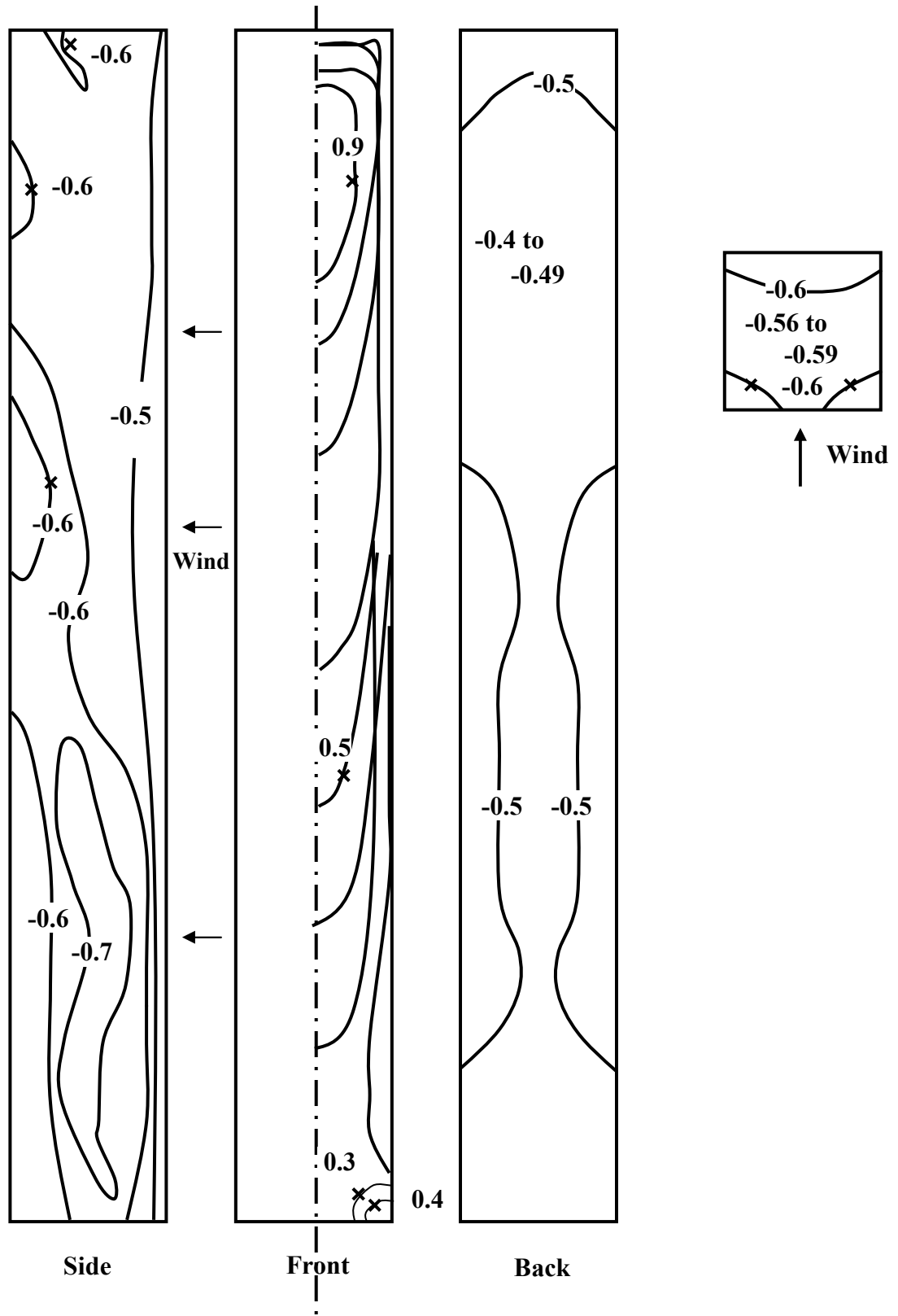


Fig. 4: Wind-tunnel measurements of the pressure coefficient on a tall building for a shear inflow perpendicular to the building face (modified from Baines, 1963).

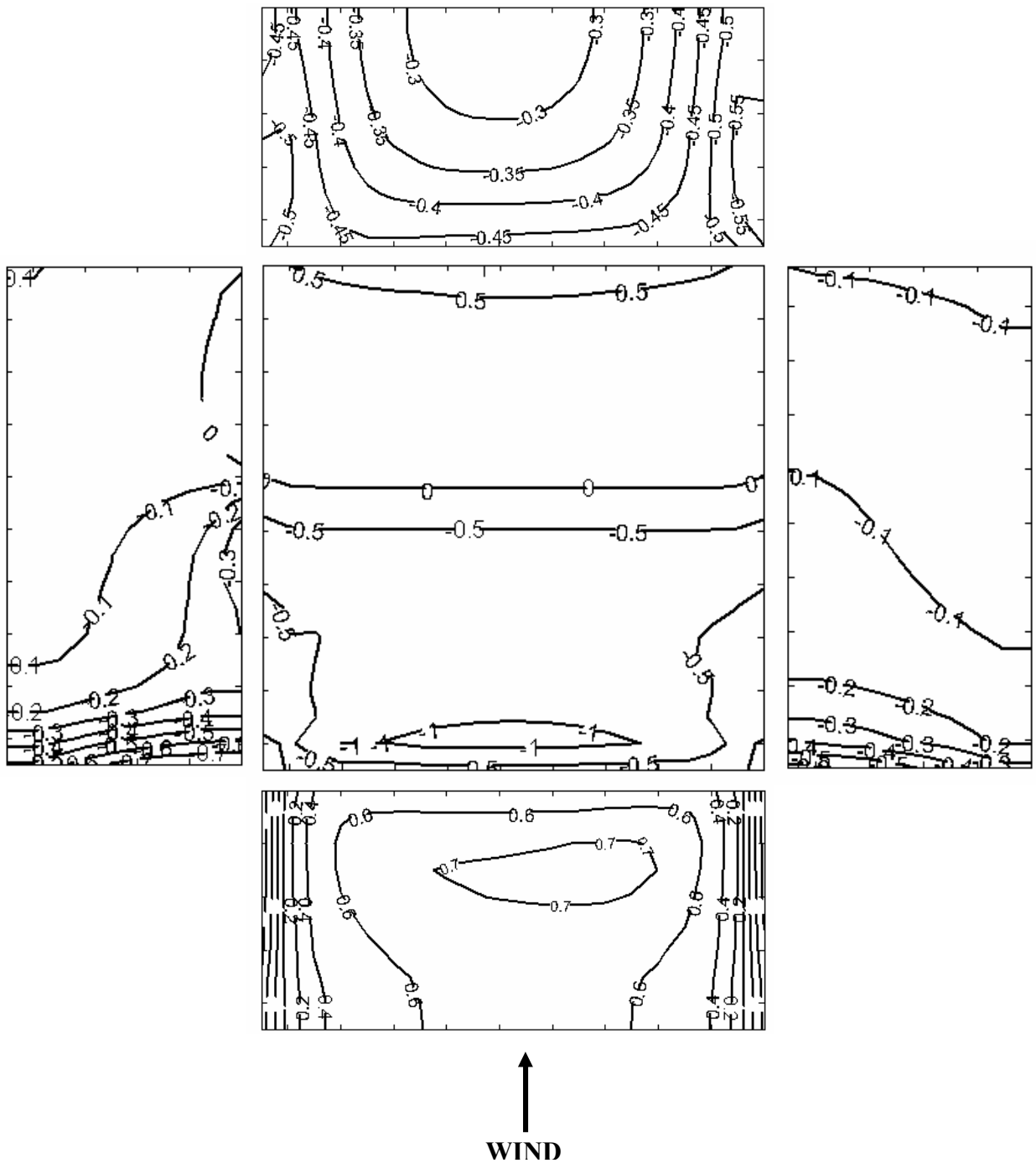


Fig. 5: Pressure coefficient produced by the QUIC Pressure Solver on a low-flat building for a shear inflow perpendicular to the building face.

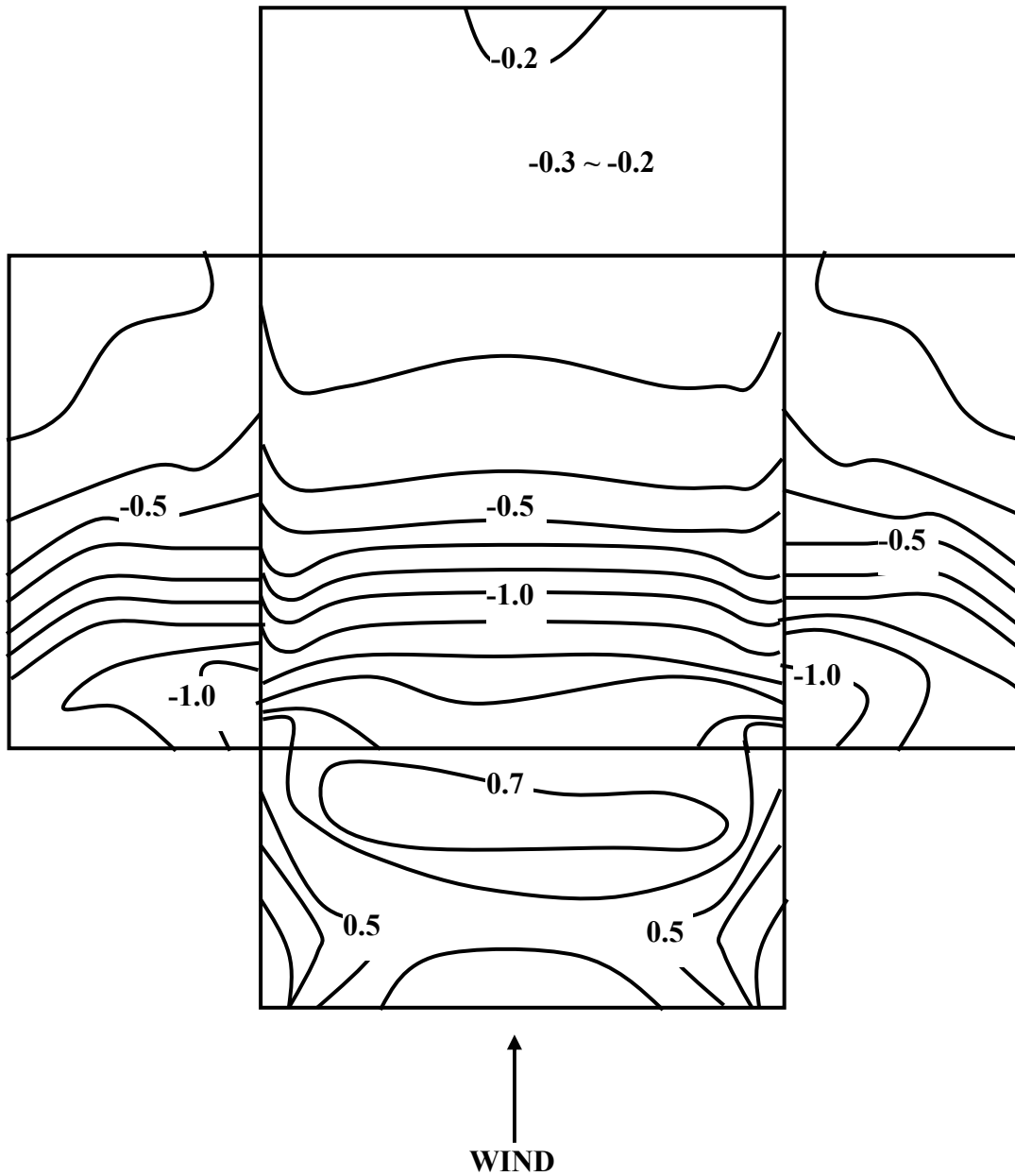


Fig. 6: Wind-tunnel measurements of the pressure coefficient on a low-flat building for a shear inflow perpendicular to the building face (modified AIJ Report, 1998).

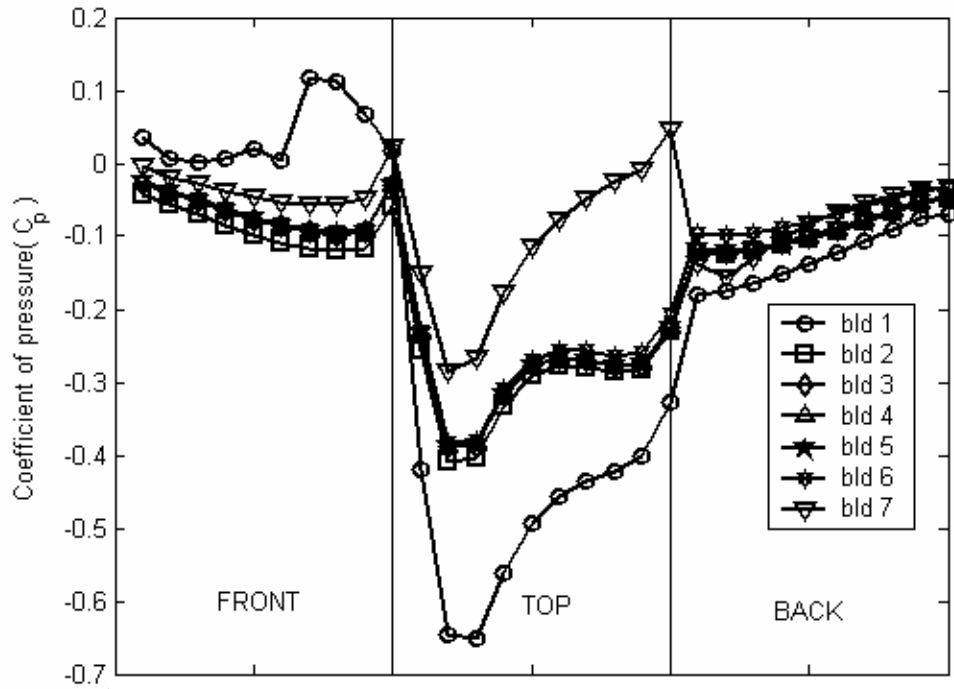


Fig. 7: Contours of pressure coefficient produced by QUIC Pressure solver on the building surfaces for sheared flow over a 2D array of 7x1 buildings.

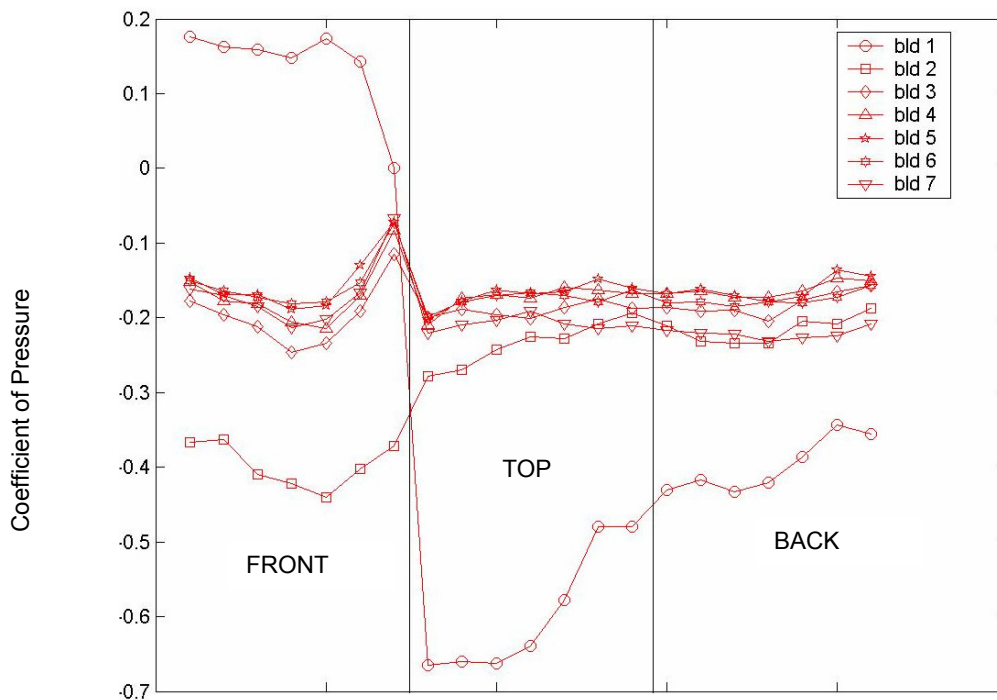


Fig. 8: Wind tunnel measurements of pressure coefficient for a sheared flow over a 2D array of 7x1 buildings (Brown et.al, 2000).